Advances in Intelligent Systems Research, volume 168

International Conference on Modeling, Analysis, Simulation Technologies and Applications (MASTA 2019)

Numerical Study on Influence of Oriented Groin Angle on Hydraulic Characteristics of Curved Water Flow

Zhou-bin CHEN, Xiao-ting ZHENG and Liang-duo SHEN*

College of Port and Transportation Engineering, Zhejiang Ocean University, Zhoushan, 316022, China

*Corresponding author

Keywords: Spur dike, Jet angle, Bend flow, MIKE3 FM model, Flow field structure.

Abstract. After the spur dike is laid in the curved channel, the water flow characteristics are significantly different with the angle of the installation. To explore this problem, by using MIKE3 FM within 60°bend channel model of single spur dike to choose different angle to the three-dimensional numerical simulation of flow around the situation and the different angle, corner the flow field structure and surface morphology analysis, such as flow is discussed in this paper. The results show that: When the angle of the spur dike is increased, the flow field structure and surface morphology around the spur dike will change. Mainly in the area of the recirculation zone after the dam, first increase and then decrease. The transverse gradient of the water surface in the upstream area increases first and then decreases. The transverse gradient of the water surface in the downstream area decreases first and then increases.

Spur dike is a commonly used building in revetment works and waterway remediation, which has the functions of protecting bank embankment, bunching water to channel, improving waterway conditions, maintaining river facies and guaranteeing diversification of aquatic environment. At present, the analysis of the characteristics of the water flow around the spur dike mainly through the river model test and numerical simulation. Kang [1] used LES (large eddy simulation) method to study and analyze the three-dimensional flow field near the rectangular spur dike in the straight channel water tank, and also analyzed the water flow structure before and after the spur dike. Outllon et al. [2] used a standard k ε–model to simulate Holtz's spur dike test and calculate the relative length of recirculation zone. Akahori et al. [3] used a non-static pressure three-dimensional model to simulate the flow around the spur tank test of Muneta et al. Domestic Li Zhiqin, Li Hong et al [4] used a standard k ε–model coupled with the control volume method to simulate the free water surface around the spur dike, and the results are basically consistent with the measured values. In this paper, the MIKE3 FM model is used to simulate the flow recirculation characteristics of continuous non-submerged spur dike. The calculation results are in good agreement with the experimental results of Han et al. [5]. On this basis, the three-dimensional model is used to study the influence of different angles of non-submerged straight spur dike on the flow field and surface morphology around the curve in the 60° curved water flow. The research results can provide reference for channel Regulation and spur design and construction which have important theoretical value and practical engineering significance.

Mathematical Model

Control Equation

The governing equation of the three-dimensional flow mathematical model [6], as follows:

$$\frac{\partial u}{\partial x}+\frac{\partial v}{\partial y}+\frac{\partial w}{\partial z}=S \quad . \tag{1}$$

$$\frac{\partial u}{\partial t}+\frac{\partial u^2}{\partial x}+\frac{\partial vu}{\partial y}+\frac{\partial wu}{\partial z}=fv-g\frac{\partial \eta}{\partial x}-\frac{1}{\rho_0}\frac{\partial P_a}{\partial x}-\frac{g}{\rho_0}\int_z^\eta \frac{\partial \rho}{\partial x}dz-\frac{1}{\rho_0 h}\left(\frac{\partial s_{xx}}{\partial x}+\frac{\partial s_{xy}}{\partial y}\right)+F_u+\frac{\partial}{\partial z}\left(v_t\frac{\partial u}{\partial z}\right)+u_s S \quad . \tag{2}$$

$$\frac{\partial v}{\partial t}+\frac{\partial v^2}{\partial x}+\frac{\partial uv}{\partial y}+\frac{\partial wv}{\partial z}=-fu-g\frac{\partial \eta}{\partial y}-\frac{1}{\rho_0}\frac{\partial P_a}{\partial y}-\frac{g}{\rho_0}\int_z^{\eta}\frac{\partial \rho}{\partial y}dz-\frac{1}{\rho_0 h}(\frac{\partial s_{yx}}{\partial x}+\frac{\partial s_{yy}}{\partial y})+F_v+\frac{\partial}{\partial z}(v_t\frac{\partial v}{\partial z})+v_s S \quad . \tag{3}$$

In the above formula, u,v,w is expressed as the velocity component in the x,y,z direction; t indicates the time; g indicates the acceleration of gravity; the coordinates in the Cartesian coordinate system are respectively x,y,z; d indicates the static water depth; η indicates the surface water height; h indicates the total water depth ($h=\eta+d$); f indicates the Coriolis parameter, and $f=2\Omega\sin\Phi$; ρ indicates the density of water; ρ_0 indicates the reference density of water; P_a indicates the atmospheric pressure; s indicates the flow rate caused by the point source; $S_{xx},S_{xy},S_{yx},S_{yy}$ indicates the radiation stress tensor; u_s,v_s indicates the flow rate of the water around the point source; v_t indicates the vertical eddy viscosity; F_u,F_v indicates the horizontal stress.

Boundary Conditions

Flow rate in the direction, the boundary conditions of the free surface and the bottom layer are:

①.Free surface $\quad z=\eta,\frac{\partial \eta}{\partial t}+u\frac{\partial \eta}{\partial x}+v\frac{\partial \eta}{\partial y}-w=0$ (4)

②. Bed bottom $\quad z=-d,u\frac{\partial d}{\partial x}+v\frac{\partial d}{\partial y}+w=0$ (5)

Model Verification

In this paper, the experimental results of particle tracking velocity measurement in Han et al. [5] are compared with the simulation results obtained by MIKE3 model to verify the accuracy and reliability of the numerical calculation of the model.

Experimental Arrangement

The experimental model of Han et al. [5]consists of two parts: a trough and two non-submerged continuous spur dikes. The length×width×height of the trough is 40m× 3.5m×0.4m, the bottom The slope is flat. The two spur dikes are exactly the same, with a length of 2m and a width of 0.3m. The width is narrowed to 0.5m and 1.5m respectively by the black water tank, and the water depth is controlled by the height of the tailgate. The water depth in the downstream zone is controlled at 14.1 cm, and the flow condition is 30L/s. The computational geometry model used in this paper is completely consistent with the above experimental model. The vertical layering is sigma coordinates and the isometric is divided into 10 layers. The calculation time step is 3s. The bottom friction type is set to 0.025 using the secondary drag coefficient. Ignore the influence of Coriolis force. Upstream boundary conditions are set as flow rate boundary $Q_{上}$=0.03m^3/s [5], and soft start is set for 10 seconds. The downstream also takes the flow rate as the boundary condition, and the boundary condition can be calculated according to the given downstream water depth and flow rate in Han et al. [5] to obtain the downstream boundary flow rate $Q_{下}$=-0.058 m^3/s, and set the soft start time as 80 seconds.

Comparison of Results

Contrast of Overall Distribution Patterns of Flow Velocity in Plane. Figure 1 is a comparison of the overall distribution of the flow velocity plane. It can be seen from the figure that the experimental results in Han et al. [5] show the entire flow field simulated by this MIKE3 FM model

shows a clear distribution of flow velocity, which varies within the range of 0~55cm/ s, among which four flow velocity ranges are obvious. This indicates that the flow velocity distribution calculated by this MIKE3 FM model is basically consistent with the measured results in Han Et al. [5].

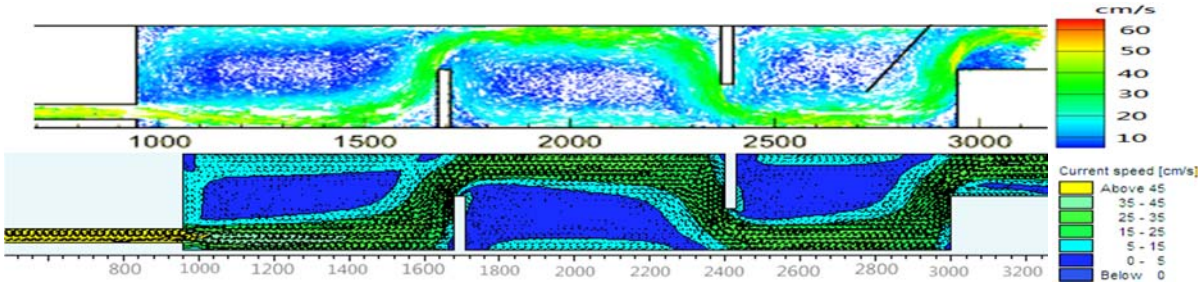

Figure 1. Comparison of the overall distribution of the velocity plane (top: measured; bottom: simulated)

Comparison of Recirculation Zones

Figure 2 is a comparison diagram of the recirculation zone division. It can be seen from the figure that the experimental results measured by Han et al. [5] can divide the recirculation zone into the main flow zone, the positive And velocity flow zone[7]. And between the positive and negative flow rates, there is a zero flow line [8]. The recirculation zone division simulated by the MIKE3 FM model is consistent with the above. And the position of the line in the upstream recirculation zone is approximately the same as the experimentally measured zero flow velocity line position. Measured in the experiment that the length of the flow increasing area is 4.2m and the length of the flow reducing area is 3.0m, While the length of the simulated flow increasing area and flow reducing area are about 4.1m and 2.9m, which are basically the same.

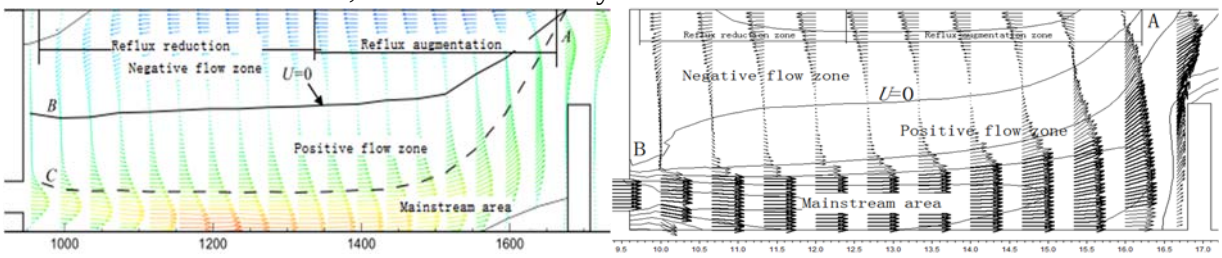

Figure 2. Comparison of the recirculation zone division (left: actual measurement; right: simulation)

Through the comparative analysis of the above two aspects, it can be proved that the simulation results of the reflow characteristics near the non-submerged spur dike are accurate and reliable by using the MIKE3 FM model.

Model Application

Research Object

This article applies the above model to study on the influence of the spur jet angle θ (the intersection angle of the tangential direction of the spur dike and the axis of the spur dike) on the hydraulic characteristics of the curved channel. The curved river spur dike arrangement is shown in Figure 3 (with θ=90° as an example). The corner of the curve is 60°, and the rectangular cross section is used. The width is 1.0m and the height is 0.4m. Setting to 4.0m transition straight section for each entrance and exit of the curve. The bending radius of convex bank side is 0.8m, and that of concave bank side is 1.8m. The spur dike is laid on the concave bank of the 30° section of the center of the curve, with a height of 0.4 m and a length of 0.4 m and a thickness of 0.06 m. Three kinds of spur dikes with θ equal to 30°, 90°and 150° are laid out. Initial water depth is 0.25m. In order to accurately analyze the change of water level in the curve, a calculation cross-section is arranged every 20° along the trend direction of the curve water. Total of 4 are arranged.

Calculation Parameters and Boundary Conditions

Using an unstructured triangle mesh and encrypting the mesh near the spur dike. The grid spacing increases gradually along the entrance and exit of the river, centering on the 30 degree section of the bend. The calculation grid design of the model under the condition of θ=90° is shown in Fig. 4 The number of calculated grid cells is 18080, the number of nodes is 9349. The vertical layering is sigma coordinates and the isometric is divided into 10 layers. The calculation time step is 0.005s.The eddy current coefficient is set to 0.28. Wall roughness is set to 0.01m. Ignored the influence of Coriolis force. The model is given two boundary conditions of upstream and downstream. The upper boundary adopts flow control, that is, Q=0.05m3/s, and the lower boundary adopts water level control, that is, the water level is 0.28m.

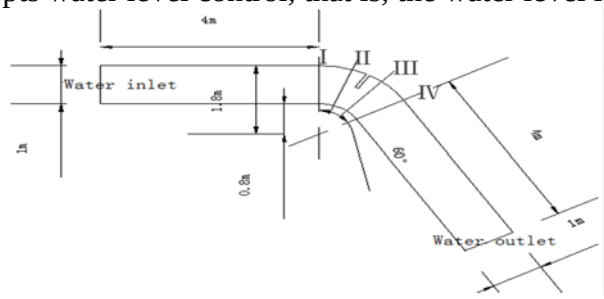

Figure 3. The layout of spur dikes in curved rivers

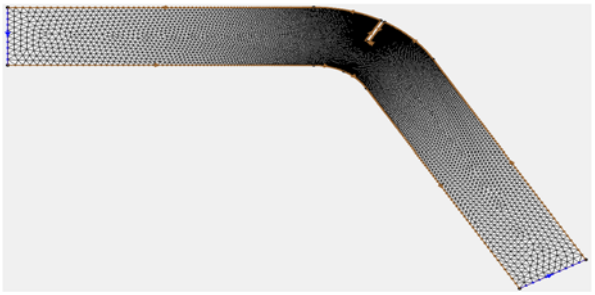

Figure 4. Mesh plotting

Analysis of Results

The Influence of Oriented Groin Angle on the Flow Field of the Curved Channel

Figure 5 and Figure 6 are the longitudinal velocity contour maps and flow field distribution diagrams of the fifth layer in the calculation of the curve under different jet angle. The flow field characteristics near the spur dike can be clearly observed from the figure, including the main flow zone and the recirculation zone. The maximum flow rate in the main flow area appears near the center .The maximum negative velocity in the backflow area the concave bank and the center of the vortex. Table 1 shows the maximum positive/ negative flow velocity under three conditions. You can see from the table that the maximum value of the maximum flow velocity value appears in the condition of laying 90° spur dike, which is about 34.58cm/s. In contrast, the minimum value is about 27.23 cm/s under the condition of 150° spur dike, which indicates that the flow is smooth under this condition. As the angle of the spur dike increases, the maximum flow velocity increases first and then decreases. The maximum may velocity near 90°.As for the maximum negative flow velocity value, the maximum value is 24.05cm/s, which occurs under the condition of laying 30° spur dam. The minimum value is 12.40cm/s, which occurs under the condition of laying 90° spur dam. Compared with the other two working conditions, this kind of Working condition is more conducive to sediment deposition in the concave bank dam field.

Table 1. Maximum positive/negative velocity table

Flow velocity type	Bucket angle		
	θ=30°	θ=90°	θ=150°
Maximum positive flow velocity [cm/s]	34.0973	34.5838	27.2253
Maximum negative flow velocity [cm/s]	-24.0535	-12.4016	-12.4525

By comparing the distance from the spur vortex in the recirculation zone behind the dam, it is found that the vortex is farthest from the dam foundation when the 90° spur is laid which the impact on the safety of the spur dike is relatively small. And roughly conforms to the following rules. When θ is less than 90°, the distance of the vortex from the dam base increases with the increase of the angle. Conversely, when θ is greater than 90° the distance of the vortex from the dam base gradually decreases as the angle increases. It can be clearly seen from the figure that the length and width of the recirculation zone change with the continuous change of θ, and the variation law is

basically consistent with the vortex .Within 90°, the larger θ is, the larger the area of reflux zone is. Outside 90°, with the increase of θ , the area of reflux zone decreases gradually and reaches a peak near $\theta = 90°$.

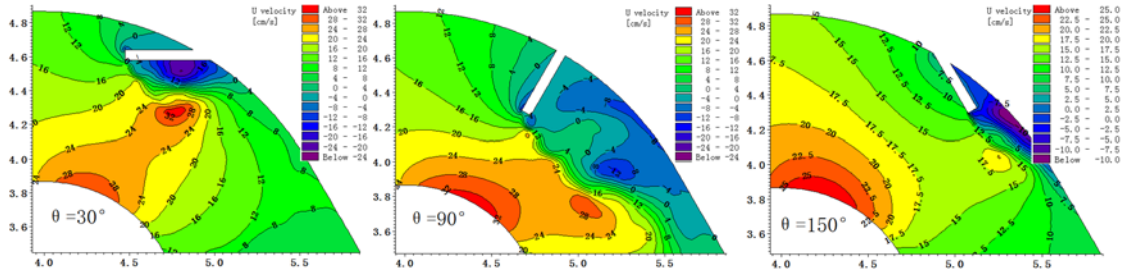

Figure 5. Planar longitudinal velocity distribution at different working conditions at bend z=0.125 m height

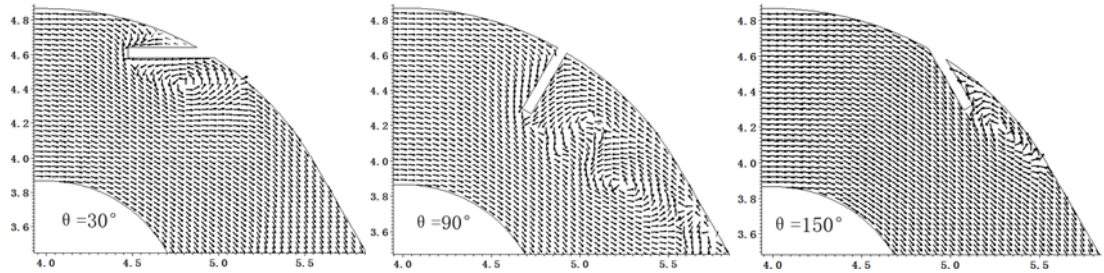

Figure 6. Flow field distribution in different working conditions at bend

The Influence of Oriented Groin Angle on the Water Surface Morphology of Curved Channel

Figure 7 is a contour map of the water level under different working conditions. It can be seen from the figure that the water surface shape inside the curve is obviously different when the spur dike is laid with different angles. Due to the layout of the spur dike, local backwater will occur in front of the spur dike, resulting in a larger water level. In the recirculation zone behind the dam and the convex bank of the curve, the water level is relatively small. When the 90° spur dike is laid, the ratio of the width of the dam to the river channel is larger. The local dammed water area in front of the spur dike is larger and the height of dammed water is the largest, which is about 0.024m. This shows that under this kind of working condition, the water blocking effect of spur dike is the strongest. At the same time as the influence on the surface morphology is maximized, the pick-up effect is also the strongest. When the 150° spur dike is laid, the dammed water phenomenon in front of the spur dike is not so obvious, and the drowning height is about 0.013m. Moreover, the range of pick-up is small and the protection effect on the concave bank is limited. Through comparative analysis, it can be concluded that the height of backwater in the upstream area of the spur dike varies with the change of jet angle. When θ is small, both the height of dammed water and the range of dammed water are small. As θ growing, the height and range of the backwater increase accordingly, and the extreme value is reached near θ=90°. Then, when θ is greater than 90°, the height and range of the backwater decrease as θ increases.

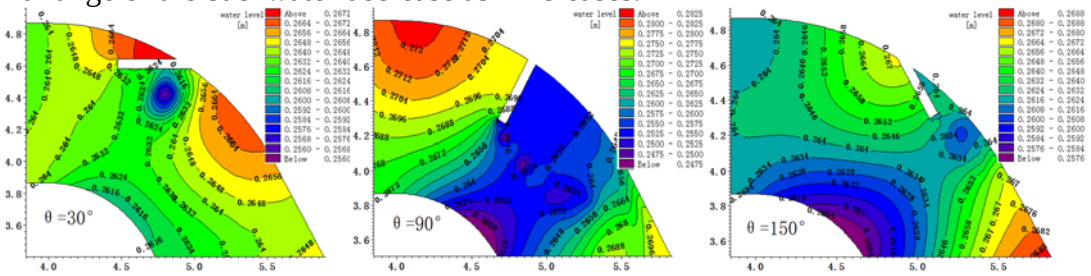

Figure 7. Isogram of water level at bend under different conditions

The transverse gradient of the water surface(J_n) is the important flow parameter of the curved river. In this paper, the formula for calculating the transverse gradient of the water surface is related to Zhang Hongwu et al. [9] and Sun Yi et al. [10].

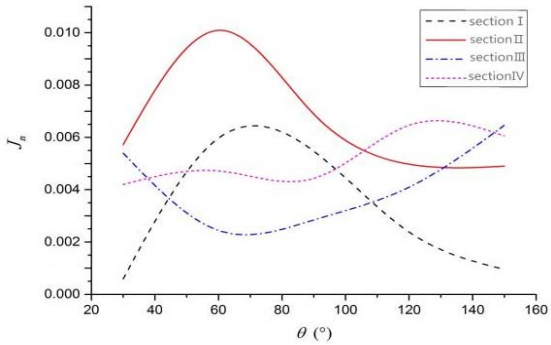

Figure 8. Distribution of the transverse gradient of the water surface of each section under different θ

Figure 8 is a plot of the water surface transverse ratio drop distribution of each section under different working conditions. According to the analysis of the figure: the water level on the side of the curved dam is always higher than the water level on the opposite side. The water surface ratio of section I and section II is basically the same as the change of the angle of the spur horn at the upper reaches of the spur. The horizontal gradient ratio increases sharply with the increase of the angle of the pick, and reaches the extreme value within 60° to 80°. Then as the angle of the pick continues to increase, the horizontal gradient ratio decreases gradually, but the transverse ratio of section II is always greater than that of section I. And this is because Section II is closer to the spur dike. The water surface ratio is sharply increased because the dam body blocks the inertial movement of the water flow. At the same time, the closer to the spur dike, the more obvious the phenomenon of dammed water, which leads to the greater the horizontal gradient ratio. Section III is located in the downstream of the spur dike. The recirculation area behind the dam is smaller when the angle of the spur dike is small. At this time, the section III is not in the recirculation zone, resulting in a large horizontal gradient ratio. And along with the changes of angle increasing, cross section III gradually influenced by reflux zone and the vortex which behind the dam. The range of the recirculation zone is first increased and then decreased, thereby causing the horizontal gradient ratio of the cross-section III to decrease first and then increase. The variation of the horizontal gradient ratio of section IV is smaller and the trend of change is more gradual. This is because the section IV is far from the spur dam and is at the exit of the curve, which causes the recirculation zone behind the dam to have less influence on the horizontal gradient ratio of section IV. It can also be analyzed according to Fig. 8 that when the oriented groin angle is between 100° and 120°, the horizontal gradient ratio of the four sections are relatively close. It shows that it is beneficial to adjust the the transverse gradient of the water surface and make the flow in the curve more stable when the 100° to 120° spur dam is deployed.

Conclusion

In this paper, the MIKE3 FM model is used to simulate the flow of curved water. The influence of the spur angle on the water flow of 60° curve is studied. After comparison and analysis, the following conclusions can be drawn. Changing the picking angle θ of the spur dike, the reflow scale at the rear of the spur dicus will also change. When θ is less than 90°, as the θ increases, the range of the recirculation zone gradually increases and the center of the vortex gradually becomes farther away from the dam. When θ is greater than 90°, as the θ increases, the range of the recirculation zone will gradually shrink and the center of the vortex gradually approaches the dam, which has an impact on the safety of the dam. At the same time, changing the picking angle θ of the spur dike can adjust the transverse gradient of the water surface near the spur dike. With the increase of θ, the transverse gradient of the water surface of the upstream of spur area increases first and then decreases, while the transverse gradient of the water surface of the downstream area of spur decreases first and then increases.

Acknowledgments
The work was financially supported by the National Natural Science Foundation of China (Grant Nos. 51879237), General Scientific Research Projects of Zhejiang Education Department (Grant Nos. Y201839488), General Projects of Zhoushan Science and Technology Bureau (Grant Nos. 2019C21026) and Zhejiang university students' science and technology innovation activity plan (Grant Nos. 2018R411014).

References

[1] KANG S,Large -eddy simulation study of turbulent flow around a rectangular spur dike, C.E3S Web of Conferences, EDP Sciences.40(2018): 05013.

[2] Ouillon S, Dartus D, Three-demensional computation offlow around groyne, J. Journal of Hydraulic Engineering .123(11) (1997)962-970.

[3] AkahoriR, Schmeeckle M, Numerical analysis of secondary –flowaround a spur dike using a three-demensional free water surface LESmodel, C. River, Coastal and Estuarine Morphodynamics. RCEM2005.

[4] Zhi-qin LI, Hong LI, Jia LI, Ran LI, Experimental study and numerical simulation of flow in the vicinity of a submerged spur-dike,J. Journal of Hydraulic Engineering. 08(2003)53-57.

[5] Han HAN, Man ZHANG, Bin-liang LIN, Jian-jun ZHOU, Experiment on flow circulations behind spur dikes, J. Journal of Hydroelectric Engineering. 36(10)(2017)84-92.

[6] Long MEI, Application Research Based on MIKE Model in Inland River Channel Renovation,D. Chongqing Jiaotong University.2014.

[7] Zhi-cong CHEN, Peng-fei HEI, Xiang DING, Division and flow scale investigation of circulation zone around spur dike,J. Advances In Water Science. 19(05) (2008)613-617.

[8] Chun-ming FANG, Yun-zhong LI, Lan-hua NIU, Liang TAN, Numerical simulation of sedimentation deposition in access channel of temporal shiplock in Three Gorges Project, J. Journal of Hydraulic Engineering. 37(3) (2006) 320-324.

[9] Hong-wu ZHANG, Xin LV, The Curved hydraulics, Water Resources and Electric Power Press, Bejing, China, 1993.

[10] Yi SUN, Xiao-e ZHAO, Xie-kang WANG, Experimental study on response characteristics of curved water flow to downstream backwater, J. Advances in Water Science.21(5) (2010)600-605.